Accepted Manuscript

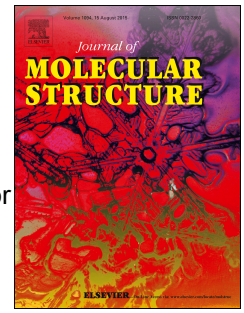

Novel thiourea derivative and its complexes: Synthesis, characterization, calculation of molecular orbitals, thermal and electrochemical behavior, antioxidant and antitumor activities

Tuncay Yeşilkaynak, Harun Muslu, Celal Özpınar, Fatih Mehmet Emen, Ruken Esra Demirdöğen, Nevzat Külcü

PII: S0022-2860(17)30491-X

DOI: 10.1016/j.molstruc.2017.04.049

Reference: MOLSTR 23672

To appear in: *Journal of Molecular Structure*

Received Date: 15 November 2016

Revised Date: 7 April 2017

Accepted Date: 12 April 2017

Please cite this article as: T. Yeşilkaynak, H. Muslu, C. Özpınar, F.M. Emen, R.E. Demirdöğen, N. Külcü, Novel thiourea derivative and its complexes: Synthesis, characterization, calculation of molecular orbitals, thermal and electrochemical behavior, antioxidant and antitumor activities, *Journal of Molecular Structure* (2017), doi: 10.1016/j.molstruc.2017.04.049.

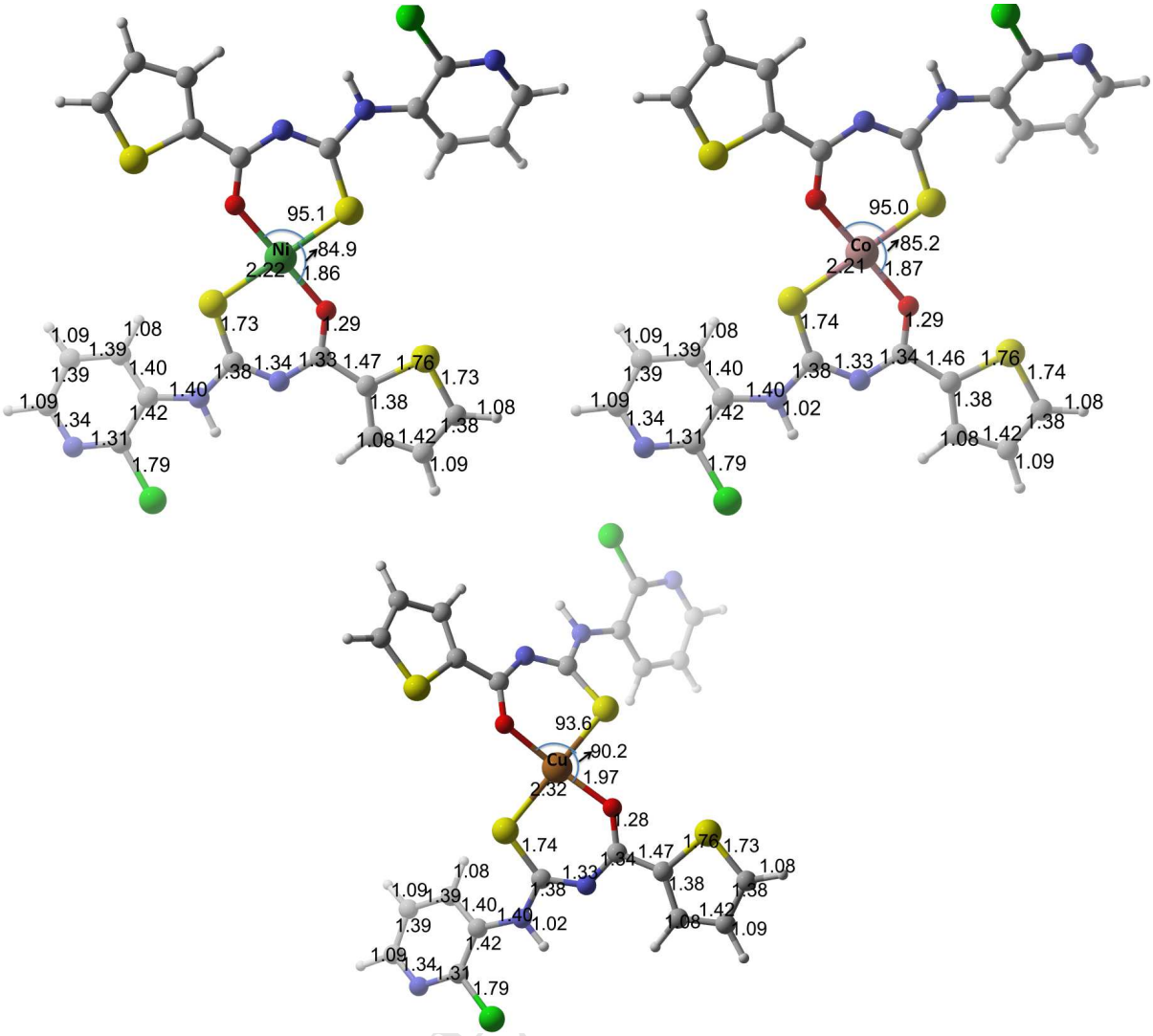
95.1
Ni
84.9
2.22
1.86
1.73
1.29
1.09
1.08
1.39
1.39
1.40
1.09
1.34
1.42
1.31
1.79
1.38
1.34
1.33
1.47
1.76
1.73
1.38
1.08
1.08
1.42
1.38
1.09
95.0
Co
85.2
2.21
1.87
1.74
1.29
1.09
1.08
1.39
1.39
1.40
1.09
1.34
1.42
1.31
1.79
1.40
1.38
1.02
1.33
1.34
1.46
1.76
1.74
1.38
1.08
1.08
1.42
1.38
1.09
93.6
Cu
90.2
1.97
2.32
1.28
1.74
1.08
1.09
1.39
1.40
1.39
1.42
1.09
1.34
1.31
1.79
1.38
1.40
1.02
1.33
1.34
1.47
1.76
1.73
1.08
1.38
1.38
1.08
1.42
1.09

Novel thiourea derivative and its complexes: Synthesis, characterization, calculation of molecular orbitals, thermal and electrochemical behavior, antioxidant and antitumor activities

Tuncay Yeşilkaynak[1], Harun Muslu[1], Celal Özpınar[2], Fatih Mehmet Emen[3], Ruken Esra Demirdöğen[4], Nevzat Külcü[5]

[1]Afsin Vocational School, Sütcü İmam University, TR46500, Kahramanmaras, Turkey
[2]Department of Chemistry Technology, Biga Vocational School,Çanakkale Onsekiz Mart University, Biga TR17200 Çanakkale, Turkey
[3]Department of Chemistry, Faculty of Arts and Science, Mehmet Akif Ersoy University,TR15030, Burdur,Turkey
[4]Department of Chemistry, Faculty of Science, Çankırı Karatekin Üniversitesi,TR18100, Çankırı,Turkey
[5]Department of Chemistry, Faculty of Arts and Science, Mersin University,TR33343, Mersin,Turkey

Abstract

A novel thiourea derivative, N-((2-chloropyridin-3-yl)carbamothioyl) thiophene-2-carboxamide,$C_{11}H_8ClN_3OS_2$ (HL) and its Co(II), Ni(II) and Cu(II) complexes (ML_2 type) were prepared and characterized by elemental analysis, FT-IR ,^{1}H-NMR and HR-MS methods. The crystal structure of HL was also investigated by single crystal X-ray diffraction study. The HL crystallizes in the orthorhombic crystal system with $P\ 2_1\ 2_1\ 2_1$ space group, Z=4, a=3.8875(3) Å, b=14.6442(13) Å, c=21.8950(19) Å. The [ML_2] complex structures were optimized by using B97D/TZVP level. Molecular orbitals of HL ligand were calculated at the same level. Thermal and electrochemical behaviors of the complexes were investigated. Anticancer and antioxidant activities of the complexes were also investigated. Antioxidant activities were determined by using DPPH (2,2-diphenyl-1-picrylhydrazyl) and ABTS (2,2′-azinobis-(3-ethylbenzothiazoline-6-sulfonic acid) assays. Anticancer activities were studied via MTT (3-(4,5-dimethylthiazol-2-yl)-2,5-diphenyltetrazolium bromide) assay in MCF-7 (Michigan Cancer Foundation-7) breast cancer cells.

Keywords: Thiourea complex; Single crystal structure; Molecular orbital; B97D/TZVP ; Thermal behavior

Corresponding Author: tyesilkaynak@ksu.edu.tr

1. Introduction

Thioureas and their metal complexes are being studied for a long time. Synthesis of thiourea compounds is facile. They have remarkable potential use as highly selective reagents for metal extraction [1]. In these type complexes, the metal ions are surrounded with S and O terminal atoms of the benzoylthioureas over a hexagonal ring chelate. The delocalization occurs for the free pair of electrons on S, O and N in hexagonal ring. Thiourea derivatives show high bioactivity characteristics against to solid tumors. Previous studies showed that benzoylthiourea complexes have antibacterial, antifungal, antithyroid, antitubercular and insecticidal properties [2-4]. Benzoylthioureas have been reported as extractants for some transition metals [5, 6]. In previous studies, metal complexes of benzoylthiourea derivatives were synthesized and their properties were reported [7–9]. Hence, in present study we focused on synthesis, characterization and elucidating the crystal structure of new thiourea derivative ligand (Figure 1) and its metal complexes. Quantum chemical computations were made to investigate molecular orbitals of the HL ligand and optimized geometries of the ML_2 complexes. We investigated thermal behavior, antioxidant and anticancer activity of metal complexes and electrochemical behavior of the Cu complex.

2. Material and Methods

2.1. Experimental

2.1.1. Synthesis of the HL Ligand

A solution of an appropriately substituted thiophene carboxylic acid chloride (0.01 mol) in acetone (50 mL) was added dropwise to a solution of KSCN (0.01 mol) in acetone (30 mL). The reaction mixtures were heated under reflux for 30 min and then cooled to room temperature. 3-amino-2-chloropyridine (0.01 mol) in acetone (10 mL) solution was added into cooled down reaction mixture. The reaction mixture was stirred for 2 h. Then, the mixture was poured onto HCl (0.1 N, 300 mL) and filtered. The obtained solid product was washed with pure H_2O and re-crystallized by using C_2H_5OH/CH_2Cl_2 according to a method given by H. Arslan, et al., 2003 [10].

N-((2-chloropyridin-3-yl)carbamothioyl)thiophene-2-carboxamide, HL: White. Yield: 84%, m.p. 161–163 ^oC. Elemental analysis, *found*: C, 44.3; H, 2.5; N, 14.0; S, 21.5; $C_{11}H_8ClN_3OS_2$ *calc*.: C, 44.4; H, 2.7; N, 14.1; S, 21.5%. FT-IR (ATR, cm^{-1}): υ(N-H) 3105, υ(C-H *aro*.)

3062, υ(C=O) 1660 (s), υ(C=S) 1165, υ(C-Cl) 745. ^{1}H-NMR (400 MHz, $CDCl_3$, ppm): 8.31 (s, 1H, N-H), 7.37–7.22 (m, 6H, Ar-H).

2.1.2. Synthesis of the [ML_2] complexes

The complexes were synthesized using the following procedure at room temperature. $MCl_2.xH_2O$ (0.001 mol) (M:Co^{2+}, Ni^{2+} and Cu^{2+}) in ethanol (10 mL) were added to the ligand (0.002 mol) in ethanol (40 mL) under constant stirring in 30 min. At the end of the synthesis procedure, the precipitate was filtered, washed with cold ethanol and dried in desiccator (Eq.1) [11].

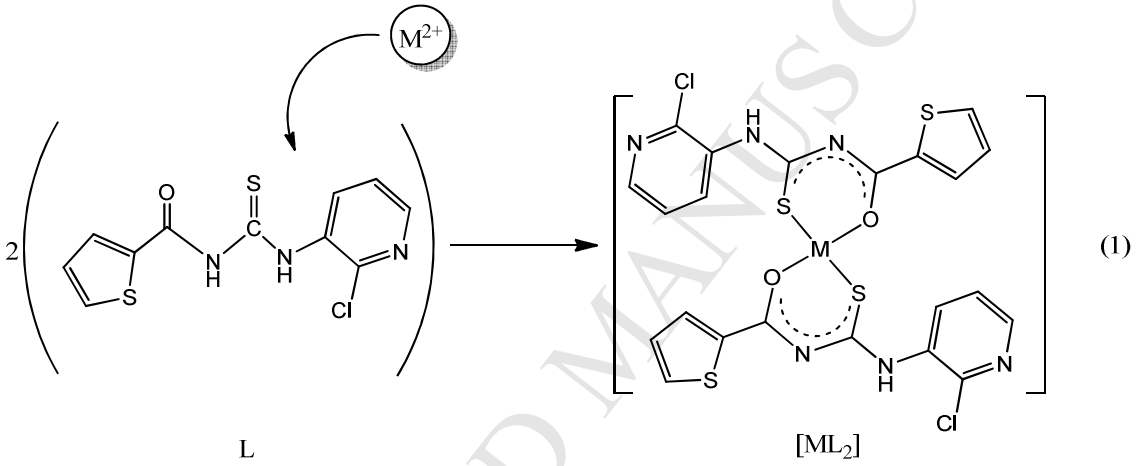

L [ML_2] (1)

Bis(N-((2-chloropyridin-3-yl)carbamothioyl)thiophene-2-carboxamide) cobalt(II), [CoL_2]: Green. Yield: 78%. Elemental analysis, *found*; C, 41.6; H, 2.1; N, 13.2, S, 20.5; $C_{22}H_{14}Cl_2N_6O_2S_4Co$ *calc.*: C, 41.3; H, 2.2; N, 12.9; S, 19.7%. FT-IR (ATR, cm^{-1}): υ(C=N) 1505 (s). HR-MS (ES^+), *m/z* (calc./found): 652.4847/652.4958.

Bis(N-((2-chloropyridin-3-yl)carbamothioyl)thiophene-2-carboxamide) nickel(II), [NiL_2]: Pale green. Yield: 82%. Elemental analysis, *found*: C, 41.0; H, 2.2; N, 13.1, S, 20.3; $C_{22}H_{14}Cl_2N_6O_2S_4Ni$, *calc.*: C, 40.9; H, 2.2; N, 12.9; S, 19.7%. FT-IR (ATR, cm^{-1}): υ(C=N) 1522 (s). ^{1}H-NMR (400 MHz, $CDCl_3$, ppm): 7.21–6.93 (m, 12H, Ar-H), 4.29 (m, 1H, N-H). HR-MS (ES^+), *m/z* (calc./found): 652.2450/652.2534.

Bis(N-((2-chloropyridin-3-yl)carbamothioyl)thiophene-2-carboxamide) copper(II), [CuL_2]: Green. Yield: 77%. Elemental analysis, *found*: C, 42.1; H, 2.3; N, 12.5, S, 20.1;

$C_{22}H_{14}Cl_2N_6O_2S_4Cu$, *calc.*: C, 41.8; H, 2.2; N, 12.7; S, 19.5%. FT-IR (ATR, cm^{-1}): υ(C=N) 1573 (s). HR-MS (ES^+), *m/z* (calc./found): 657.0976/657.1060.

2.2. Instrumental

^{1}H-NMR spectra were studied on a Bruker Avance III 400 MHz NMR spectrometer. ^{1}H-NMR studies were made by using $CDCl_3$ as solvent and TMS as internal standard. ^{1}H-NMR signals were recorded. Perkin Elmer LX-125000B FT-IR spectrophotometer with ATR component (4000–30 cm^{-1}) was used to obtain FT-IR spectra. Elemental analyses were made on a Costech ECS 4010 instrument. Melting points of the ligands were determined via Stuart model SMT30. Mass studies were made via Waters SYNAPT G1 MS instrument. The positive mode (ES+) with HR-MS (Da 50-1000, ESI-TOF-MS) was used for exact mass analysis. Single crystal X-ray data of the HL were collected on a Bruker D8 Venture diffractometer by using monochromated MoK_α radiation. The structure was solved and refined using Bruker SHELXTL Software. The structure of the HL was solved by direct methods and refined on F^2 by full matrix least-squares using SHELXL 2013[22]. All non-hydrogen atoms were refined with anisotropic displacement parameters. The molecular structure plots were prepared by using Mercury CSD 2.4 [23]. TG/DTA analyses were carried out on a SEIKO-II instrument. The thermal decomposition behaviors of the complexes were investigated at a heating rate of 10 °C min^{-1} under N_2 atmosphere via DTA/TG. The cyclic voltammetric measurements using glassy carbon electrode were carried out by using a BAS 100 W (Bioanalytical System, USA) electrochemical analyzer. A glassy carbon working electrode (BAS; *Φ*: 3 mm diameter), a Ag/AgCl reference electrode (BAS; 3 M KCl) and platinum wire counter electrode were used. The standard one-compartment three electrode cell was used in all experiments. The cyclic voltammogram plots were taken at room temperature.

2.3. Computations

In this study, computations were made by using G09 [12] program package. HOMO and LUMO orbitals of the ligands were computed as single point calculation by using B97D/TZVP [13,14] level on the X-ray structure. DOS (density of state) spectrum was obtained by using Gaussum [15] program package. The proposed $[ML_2]$ complex structures were optimized by using the same computational level. The optimized bond distances and

angles were visualized by using CYLView[16] program package. Frequency calculations were made to verify that optimized structures are stationary points with no imaginary frequency.

3. Results and Discussion

3.1. FT-IR studies

FT-IR studies were made to identify the types of bonds in the ligand and its metal complexes. In the FT-IR spectra of the HL broad vibration bands are observed at 3105 cm^{-1} and 3320 cm^{-1} which indicate the N-H groups. The sharpest peak observed at 1660 cm^{-1} belongs to the stretching vibration of the carbonyl group in the HL. It was observed that the vibration band of the C=O and C=S disappeared after the complex formation reaction. At the same time, a new peak appeared in the 1470–1520 cm^{-1} range, which can be attributed to the absorption of C–N stretching vibration band. In the spectra of the complexes, there is another intense absorption band at 848–858 cm^{-1} corresponding to the C–S fragment. The stretching vibration band of the C=S group was observed at 1165 cm^{-1}. The shifted vibration band of the C=S group in the complexes cannot be observed because of overlapping with other bands in that region.

When HL is attached to metal, deprotonation occurs. So the stretching vibration band of the N-H group (3320 cm–1) cannot be observed in the FT-IR spectra of the metal complexes. HL it is bonded to the metal atom (Table 1). The peaks of the C-Cl group in the compound are observed in the range 740-745 cm-1. Disappearance of the N–H band and shifting of the C=O and C=S bands confirmed formation of the complexes. These results are appropriate with our previous results [10,17-21]. The C–S , C–O and C–N stretching bands were also computed with B97D/TZVP for the complex structures. Theoretical calculations show the stretching vibration bands of the C-S, C-O and N-H groups at 1180 cm^{-1}, 874 cm^{-1} and 3474 cm^{-1}, respectively. The selected vibrational bands can be seen in Table 2 and the theoritical IR spectrum of the [NiL_2] is also shown in Figure 2.

3.2. ^{1}H-NMR Studies

The molecular structures of the ligand and [NiL_2] complex were also described by H^1-NMR method. In ^{1}H-NMR spectrum of the HL, the observed peaks at 8.29-8.31 ppm can be attributed to the N-H group. The aromatic C-H groups in HL appear as multiple peaks at 7.37-7.22 ppm. Another N-H peak is also observed at 4.34 ppm. The N-H peaks, which are observed at 8.29-8.31 ppm, did not appear in the [NiL_2]. These results are affirmative of the complexation reaction. The other N-H peak and aromatic C-H protons in the [NiL_2] appeared at 4.29 ppm and 7.21-6.93 ppm respectively. ^{1}H-NMR spectra of the [CoL_2] and the [CuL_2] complexes could not be obtained because of their paramagnetic properties.

3.3. Crystal structure analysis of the HL

The crystal and instrumental parameters were used to the unit-cell determination and data collection is summarized in the supporting information. Molecular structure scheme of the HL is given in Figure 3.

Crystal data and the structure refinement parameters of the HL are given in Table 3. The experimental geometric parameters are also given in the supporting information.

The structures were resolved and refined using the space group $P\ 2_1\ 2_1\ 2_1$, with Z = 4 for the formula unit, $C_{11}H_8ClN_3OS_2$ (HL) via Bruker SHELXTL Software Package. Specific bond lengths (Table 4) and angles (Table 5) of the HL are tabulated as below.

The bond lengths and angles in the HL are typical for the thiourea derivatives; C6-S2 and C5-O1 bonds displayed a typical double-bond character with 1,657(3) and 1,222(3) Å, respectively. The bond lengths of the N2-C6, N3-C6, N3-C5, and N2-C7 were determined to be 1,328(4), 1.392(3), 1.376(4) and 1,410(4) Å, respectively. Considering these results it could be interpreted with partial double bond character. The carbonyl and thiocarbonyl bond angles are N2-C6-S2, 119.3(2); N3-C6-S2, 118.5(2); N3-C5-O1, 122.1(3) and O1-C5-C4, 122.1(3)^{o} [17,19]. The crystal packing scheme of HL is given in Figure 4.

There is one intermolecular, N-H…O hydrogen bond. The bond length of H…O in this is 1,955 Å [10, 24, 25]. Orbital diagrams of the HL were given in Figure 5. For HL molecule,

HOMO are dominantly made up of π orbitals of the sulfur atom. On the other hand, the LUMO mainly delocalized over amide and thioamide moiety and thiophene ring of the HL molecule.

3.4. The Complex Structure

The [ML_2] (M: Ni, Co, Cu) structures were proposed based on the reported cis-Bis(*N*,*N*-dimethyl-*N*'-2-chlorobenzoylthioureato)Ni(II) crystal structure [26] and were optimized by using B97D/TZVP computational level. Figure 6 shows optimized bond distances and O-M-S bond angles of the [ML_2] structures, respectively.

The O-M-S bond angles in the [NiL_2] and [CoL_2] structures are very similar, but in the [CuL_2] they slightly differ from those of the Ni and Co complexes. While the M-O distance in the complexes follows the order Ni-O < Co-O < Cu-O the order of the M-S distance follows the order Co-S < Ni-S < Cu-S. It can be said that the bond lengths of the rest of the bond types (the C-O, C-S, C-N, C-C, and C-H bonds) are almost the same in all complex structures since the largest difference is only 0.02 Å. The C6-S2 bond distance elongates from 1.657 Å in the HL structure to 1.73 – 1.74 Å in the [ML_2] structure. Similarly, the C5-O1 bond length also stretches from 1.222 Å to 1.28 – 1.29 Å for the [ML_2]. Due to leaving proton from N3 atom, C6-N3 and C5-N3 bond lengths changed to 1.34 and 1.34 Å in the [ML_2], respectively. The elongation of C-S, C-O and C-N bonds is estimated that the coordination possibly originating from back-donating character of the ligand.

3.5. Thermal Behavior of the Complexes

The DTA/TG curves of the [CoL_2] are shown in Figure 7 and the thermo-analytical results are given in Table 6.

The TG curve reveals that the decompositions of the [CoL_2] take place in four stages. The first decomposition stage occurs in the temperature range 145–251 ^{o}C. In this step, 1/3 mol ligand was eliminated via an experimental mass loss of 16.20% (calc.~15.2%) and the intermediate product formed is given with the formula [$CoL_{5/3}$]. The second decomposition carried out between 251 and 395 ^{o}C with a mass loss of 12.10% (calc.:~11.4%). In this stage, 1/4 mol ligand was decomposed and turned into gas products and an intermediate with the [$CoL_{17/12}$] formula was formed. The third decomposition is observed between 395 ^{o}C and 587

^{o}C with a mass loss of 29.80% (calc.:~30.4%). At the end of this stage, 2/3 mol ligand left from the structure and turned the gas products and an intermediate with the [$CoL_{3/4}$] formula was formed. The last decomposition is observed at a temperature >587 ^{o}C. The remaining product is thought to be CoS [7,27]. The results obtained from TG/DTA curves are tabulated in Table 6.

Thermal decomposition reactions of the [CoL_2] are suggested to be as follows;

$$[CoL_2] \xrightarrow{145\text{-}251\ ^0C} [CoL_{5/3}] \xrightarrow{251\text{-}395\ ^0C} [CoL_{17/12}] \xrightarrow{395\text{-}587\ ^0C} [CoL_{3/4}] \xrightarrow{>587\ ^0C} CoS$$

The DTA/TG curves of the [NiL_2] are shown in Figure 8 and the results are given in Table 7. The TG curve shows that the decomposition process of the [NiL_2] occurs in three stages. The first decomposition stage occurs in the temperature range between 182–407 ^{o}C. In this step, 1/3 mol of the ligand was eliminated corresponding to an experimental mass loss of 15.10% (calc.~15.2%) and an intermediate with the formula [$NiL_{5/3}$] was formed. The second decomposition is observed between 407 and 583 ^{o}C with a mass loss of 46.30% (calc.:~45.7%) and one mol ligand was decomposed and an intermediate with [$NiL_{2/3}$] formula was formed. Then, this compound turns into NiS_2 at >583 ^{o}C with a mass loss of 21.20% (calc.:~20.3%)[18, 28, 29]. The TG/DTA results are given in Table 7.

Thermal decomposition reactions of the [NiL_2] are suggested to be as follows;

$$[NiL_2] \xrightarrow{182\text{-}407^0C} [NiL_{5/3}] \xrightarrow{407\text{-}583\ ^0C} [NiL_{2/3}] \xrightarrow{>583\ ^0C} [NiS_2]$$

The DTA/TG curves of the [$CuL^1{}_2$] are given in Figure 9 and the results are given in Table 8. The decomposition process of the [CuL_2] takes place in three stages. The first decomposition occurs in temperature range of 145–285 ^{o}C. In this step, 1/3 mol of ligand was broken up resulting in an experimental mass loss of 15.20% (calc.~15.1%). At the end of this stage, the intermediate with the formula [$CuL_{5/3}$] was formed. The second decomposition stage is observed in temperature range of 285–575 ^{o}C with a mass loss of 45.90% (calc.:~45.3%). At this stage, 1 mol ligand was seperated and turned into gas products and an intermediate with the formula [$CuL_{2/3}$] was formed. The last decomposition is observed between 575 and 935 ^{o}C and the remaining product is suggested to be $Cu_{1.96}S$ [18, 28, 29]. The TG/DTA results are given in Table 8.

Thermal decomposition reactions of the [CuL_2] are recommended to be as follows;

$$[CuL_2] \xrightarrow{145\text{-}285\ ^0C} [CuL_{5/3}] \xrightarrow{285\text{-}575\ ^0C} [CuL_{2/3}] \xrightarrow{>575\ ^0C} Cu_{1.96}S$$

3.6. Antioxidant and Antitumor Activities

The biological activities of the [CoL_2], [NiL_2] and [CuL_2] complexes were investigated by studying their antioxidant and antitumor activities in cell culture systems. The antioxidant activities were studied by using the DPPH and ABTS assays. The antioxidant activity of the complexes is proportional to DPPH, ABTS and reduction power values. The DPPH, ABTS, Reduction power and IC_{50} values are presented in Table 9.

As a result of studies, it was observed that [CoL_2] shows good antioxidant properties when compared to other complexes. These results show that antioxidant properties of the [CoL_2] are better than those of Propyl gallate and worse than those of Vitamine E [30]. The anticancer activities were studied MTT assay in MCF-7 breast cancer cells. MTT assay is an important method fast, facile and highly accurate method for determining the anticancer activity. A tetrazolium salt MTT is a yellow colored, living cells bind specifically to the succinate dehydrogenase enzyme located in the mitochondria. The amount of living cells will be determined as a function of the amount of binding via spectrophotometric method. Thiourea compounds are known to exhibit high antitumor properties[31]. In other studies, it was suggested that the external N-H of the thiourea has a better hydrogen bond interaction with the protein [32]. Besides, it suggested that compounds with strong electron-drawing groups on aromatic ring (as Cl) may benefit for the antitumor activities of compounds [32]. It is known that the low value of IC_{50} means that the antitumor property of compound is good. In this study, the results showed that the [CuL_2] also have good antitumor activity. The IC_{50} value of [CuL_2] complex have a comparable activity as 5-FU which is widely employed in the treatment of cancer. Besides other compounds (IC_{50} values, >50 ppm) were less active against the tumor cells [33]. In a similar way, the researchers examined the antitumor properties of the Cu complex. They observed that the Cu complexes showed good antitumor properties against breast tumor [34, 35].

3.7. The Electrochemical Behavior of the [CuL_2]

In previous studies, electrochemical behavior of thiourea derivatives was investigated [36, 37]. In this work, to understand electrochemical behavior of the [CuL_2], cyclic voltammetric (CV) studies were made. In the cyclic voltammogram of the [CuL_2], two peaks were observed. One of them was observed at about +0.35 V, which is an oxidation peak, and the other one was observed at about -0.50 V which is a reduction peak. pH measurements showed that the optimum medium is pH=2 (in Britton-Robinson buffer solution, BRB) since the sharpest and best peak results were obtained in this medium. To understand whether the process diffusion or absorption controlled scan rate studies were carried out between 25 mV/s and 750 mV/s scan rates. Scan rate studies were made at pH=2 in BRB, where the best oxidation reduction results were obtained. The typical scan rate curves of the [CuL_2] are given in Figure 10.

Scan rate studies were investigated between the 25-750 mV/s scan rate and at a concentration of 1 x 10^{-5} M. The linear dependence of the peak current Ip (μ) on the square root of the scan rate $v^{1/2}$ (mVs^{-1}) was found by GCE which indicated diffusional behavior. The equations regarding the scan rate studies for the [CuL_2] is give via the below equation (1);

$$\text{Log } I_p\,(\mu A) = 0,1974\,\sqrt{v}\,(mVs^{-1}) - 0,9191 \quad (r^2 = 0,9109) \qquad (1)$$

The linear relationship between Log I_p and Log v was investigated and the equations about these relationships are given via the below equation (2);

$$\text{Log } I_p\,(\mu A) = 0,5959\,\text{Log } v\,(mVs^{-1}) - 1,0703 \quad (r^2 = 0,9177) \qquad (2)$$

The slope of the relationships fit the theoretically expected values for an ideal diffusion controlled reaction (0.5) [38]. The Cu (II) complexes could be investigated since they are stable in this pH range. However, the electrochemical behavior of other complexes could not be investigated for instability [39, 40].

4. Conclusions

N-((2-chloropyridin-3-yl)carbamothioyl)thiophene-2-carboxamide, $C_{11}H_8ClN_3OS_2$ (HL), and its Co(II), Ni(II) and Cu(II) complexes were synthesized. To define the structure of HL and its metal complexes elemental analysis, FT-IR, ^{1}H-NMR and HR-MS methods were used. The HL was also characterized by single crystal X-ray diffraction study. X-ray diffraction study results showed that HL crystallizes in the orthorhombic system with *P* 2_1 2_1 2_1 space group and Z=4, and its unit cell parameters were a=3.8875(3) Å, b=14.6442(13) Å, c=21.8950(19) Å. Molecular orbitals of both HL and [ML_2] structures were optimized by B97D/TZVP level. Thermal behaviors of the complexes were investigated. The [CoL_2], [NiL_2] and [CuL_2] complexes are thermally stable up to 145, 182 and 145 ^oC, respectively. The [NiL_2] and [CuL_2] complexes were decomposed in three stages while the [CoL_2] complex was degrades in four steps. The anticancer and antioxidant activities of the metal complexes were also investigated. The antioxidant activities of the complexes were determined by using the DPPH and ABTS assays. Anticancer activities of the complexes were studied via MTT assay in MCF-7 breast cancer cells. The comparison of the results obtained with those obtained with other complexes showed that the [CuL_2] complexes had better antitumor activities. However, only the cyclic voltammograms of [CuL_2] could be obtained. Cu (II) complexes were stable in working pH range. The cyclic voltammograms of [CuL_2] showed oxidation and reduction peaks at +0.35 V and -0.50 V, respectively.

Appendix A. Supplementary material

Crystallographic data for the structure reported in this paper have been deposited at the Cambridge Crystallographic Data Centre (CCDC), CCDC 1055244 (HL). This data can be obtained free of charge from The Cambridge Crystallographic Data Centre via www.ccdc.cam.ac.uk/data_request/cif. [Fax: int code +44(1223) 336-033; e-mail: deposit@ ccdc.cam.ac.uk]. Cartesian coordinates of optimized geometries and the computed IR spectra are also available.

Acknowledgements

This work was supported by Kahramanmaraş Sütçü İmam University Research Fund (BAP-project no:2013/4-28M). We also thank TUBITAK ULAKBIM, High Performance and Grid Computing Center (TR-Grid e-Infrastructure) for the calculations.

References

[1] L. Beyer, J.J. Criado, E. Garcia, F. Lessmann, M. Medarde, R. Richter, E. Rodriguez,

Tetrahedron 52 (1996) 6233-6240.
[2] V.K. Madan, A.D. Taneja and V.P. Kudesia, Indian Chem Soc. 68 (1991)471–472.
[3] S.A.F. Rostom, Bioorganic & Medicinal Chemistry 14 (2006) 6475–6485.
[4] H.Q. Li, T. Yan, Y. Yang, L. Shi, C.F. Zhou, H.L. Zhu, Bioorganic & Medicinal Chemistry 18 (2010) 305–313.
[5] K.H. Konig, M. Schuster, G. Schneeweis, B. Steinbrech, Fresenius Z. Anal. Chem. 319 (1984) 66-69.
[6] K.H. König, M. Schuster, B. Steinbrech, G. Schneeweis, R. Schlodder, Fresenius Z. Anal. Chem. 321 (1985) 457-460.
[7] N. Ozpozan, T. Ozpozan, H. Arslan, F. Karipçin, N. Külcü, Thermochim. Acta. 336 (1999) 97-103.
[8] N. Özpozan, H. Arslan, T. Özpozan, N. Külcü, Thermochim. Acta. 343 (2000) 127-133.
[9] N. Özpozan, H. Arslan, T. Özpozan, M. Merdivan, N. Külcü, J. Ther. Anal. 61 (2000) 955-965.
[10] H. Arslan, U. Flörke and N. Külcü, J. Chem. Cryst. 33(2003) 919-924.
[11] N. Gunasekaran, P. Jerome, S.W. Ng, E.R.T. Tiekink, R. Karvembu, Molecular Catal A: Chem. 353-354 (2012) 156-162.
[12] M.J. Frisch, G.W. Trucks, H.B. Schlegel, G.E. Scuseria, M.A. Robb, J.R. Cheeseman, G. Scalmani, V. Barone, B. Mennucci, G.A. Petersson, H. Nakatsuji, M. Caricato, X. Li, H.P. Hratchian, A.F. Izmaylov, J. Bloino, G. Zheng, J.L. Sonnenberg, M. Hada, M. Ehara, K. Toyota, R. Fukuda, J. Hasegawa, M. Ishida, T. Nakajima, Y. Honda, O. Kitao, H. Nakai, T. Vreven, J.A. Montgomery, J.E. Peralta, F. Ogliaro, M. Bearpark, J.J. Heyd, E. Brothers, K.N. Kudin, V.N. Staroverov, R. Kobayashi, J. Normand, K. Raghavachari, A. Rendell, J.C. Burant, S.S. Iyengar, J. Tomasi, M. Cossi, N. Rega, J.M. Millam, M. Klene, J.E. Knox, J.B. Cross, V. Bakken, C. Adamo, J. Jaramillo, R. Gomperts, R.E. Stratmann, O. Yazyev, A.J. Austin, R. Cammi, C. Pomelli, J.W. Ochterski, R.L. Martin, K. Morokuma, V.G. Zakrzewski, G.A. Voth, P. Salvador, J.J. Dannenberg, S. Dapprich, A.D. Daniels, O. Farkas, J.B. Foresman, J.V. Ortiz, J. Cioslowski, D.J. Fox. *Gaussian*, Inc., Wallingford CT (2009).
[13] S. Grimme. J. Comp. Chem. 27 (2006) 1787-1799.
[14] A. Schaefer, C. Huber and R. Ahlrichs, J. Chem. Phys. 100 (1994) 5829-5835.
[15] N.M. O'Boyle, A.L. Tenderholt, K.M. Langner, J. Comp. Chem. 29 (2008) 839-845.
[16] CYLview, 1.0b; Legault CY. Université de Sherbrooke (2009). (http://www.cylview.org)
[17] G. Binzet, H. Arslan, U. Florke, N. Kulcu, N. Duran, J. Coord. Chem. 59 (2006) 1395-1406.
[18] D. Uğur, H. Arslan, N. Külcü. Russian J. Coord. Chem. 32 (2006) 669-675.
[19] H. Arslan, U. Florke, N. Kulcu, M.F. Emen, J. Coord. Chem. 59 (2006) 223-228.
[20] M.F. Emen, H. Arslan, N. Kulcu, U. Florke, N. Duran, Pol. J. Chem. 79 (2005) 1615-1626.
[21] H. Arslan and N. Külcü, Trans. Metal Chem. 28 (2003) 816–819.
[22] G.M. Sheldrick, Acta Cryst. Sect. A 64 (2008)112–122.
[23] C.F. Macrae, I.J. Bruno, J.A. Chisholm, P.R. Edgington, P. McCabe, E. Pidcock, L. Rodriguez-Monge, R. Taylor, J. van de Streek and P.A. Wood, J. Appl. Cryst. 41 (2008) 466–470.
[24] G. Binzet, F.M. Emen, U. Flörke, T. Yesilkaynak, N. Külcü and H. Arslan, Acta Cryst. E65 (2009) 81-82.
[25] T. Yeşilkaynak, U. Flörke, N. Külcü and H. Arslan, Acta Cryst. E62 (2006) 3934-3935.
[26] F.M. Emen, U. Flörke, N. Külcü and H. Arslan, Acta Cryst. E59 (2003) 582-583.
[27] T.S. Breviglieri, E.T.G. Cavalheiro, G.O. Chierice, Thermochim. Acta.356 (2000) 79-84.

[28] J.F.W. Mosselmans, R.A.D. Pattrick, G. van der Laan, J.M. Charnock, D.J. Vaughan, C.M.B. Henderson, C.D. Garner, Phys. Chem. Minerals 22 (1995) 311-317.
[29] G. Binzet, H. Arslan, N. Külcü, Asian J. Chem. 19 (2007) 5711-5717.
[30] Y. Dong , T.K. Venkatachalam, R.K. Narla, V.N. Trieu, E.A. Sudbeck and F.M. Uckun, Bioorg. & Med. Chem. Let. 10(1) (2000) 87-90.
[31] S.N. Manjula, N. M. Noolvi, K. V.Parihar, S.A.M. Reddy, V. Ramani, A.K. Gadad, G. Singh, N.G. Kutty, C.M. Rao, E.J. Medicinal Chem. 44 (2009) 2923-2929.
[32] H.Q. Li, T. Yan, Y. Yang, L. Shi, C.F. Zhou, H.L. Zhu, Bioorganic and Medicinal Chem. 18 (2010) 305-313.
[33] W. Liu, J. Zhou, T. Zhang, H. Zhu, H. Qian, H. Zhang, W. Huang, R. Gust, Bioorganic Med. Chem. Let. 22 (2012) 2701-2704.
[34] R. Kumar, S. Obrai, A.K. Jassal, M.S. Hundal, J. Mitra and S. Sharma, J. Coord. Chem. 68,12 (2015) 2130-2146.
[35] X.T. Zhang, Z.Y. Ma, C. Zhao, Q.J. Zhou, C.Z. Xie and J.Y. Xu, J. Coord. Chem. 68,13 (2015) 2307-2323.
[36] L.M. Gassa, J.N. Lambi, A.E. Bolza´n, A.J. Arvia, J. Electroanal. Chem. 527 (2002) 71-84.
[37] M. Yan, K. Liu, Z. Jiang, J. Electroanal. Chem. 408 (1996) 225-229.
[38] H. Muslu, A. Golcu, M. Tumer, M. Özsöz, J. Coord. Chem. 64,19 (2011) 3393-3407.
[39] K.H. König, M. Schuster, B. Steinbrech, G. Schneeweis, R. Schlodder, Fresenius Z. Anal. Chem. 321 (1985) 457-60.
[40] M. Schuster. Inaugural-dissertation Zu Erlangung des Doktorgrades der Naturwissens-ChaftenVorgelegt beim Fachbereich Chemie de Johann Wolfrang Goethe-Universitat zu Frankfurt am Main (1986).

Comp.	$\upsilon(N_3\text{-}H_4)$/ cm^{-1}	$\upsilon(N_2\text{-}H_5)$ cm^{-1}	υ(C-H) (ring)/ cm^{-1}	υ(C=O)/ cm^{-1}	υ(C=N)/ cm^{-1}	υ(C=S)/ cm^{-1}	υ(C-Cl)/ cm^{-1}
HL	3320	3105	3062	1660	-	1165	745
CoL_2	-	3095	2972	-	1505	-	745
NiL_2	-	3075	2976	-	1522	-	741
CuL_2	-	3085	2971	-	1573	-	740

Vibrations (cm^{-1})	Assignment
3474	(N – H)
3179 - 3109	$(C – H)_{arom}$
1568 – 1549	$(C – N \text{ and } C – C)_{pyridine}$
1515 - 1502	$(C – C)_{thiophene}$
1452 - 1405	$(C_{C=O} – N – C_{C=S})$
1256 - 1258	$(C – S)_{C=S}$ and $(C – O)_{C=O}$
1180	$(C – S)_{C=S}$
874	$(C – O)_{C=O}$
836	$(C – S)_{thiophene}$

Empirical formula	$C_{11}H_8ClN_3OS_2$
Formula weight(g/mol)	297.78
T(K)	299
λ(Å)	0.71073
Crystal system	Orthorhombic
Space group	*P* 2_1 2_1 2_1
Unit cell dimensions: (Å,º)	
A	3.8875(3)
B	14.6442(13
C	21.8950(19)
A	90
β	90
Γ	90
V(Å^3)	1246.47(18)
Z	4
μ (mm^{-1})	0.631
ρ (g cm^{-3})	1.587
F(000)	608
Crystal size (mm)	0.02x0.05x0.1
θ range for data collection(º)	2.32 to 25.32
Index ranges	-4≤h≤4
	-17≤k≤17
	-26≤l≤26
Reflections collected	27017
Independent reflections	2266
Coverage of independent ref.	99.4%
Data/parameters	2266/163
Max. and min. transmission	0.988/0.940
R1, wR2 [I ≥ 2σ(I)]	0.0288
	0.0558
R1, wR2 (all data)	0.0405
	0.0590
GOF on F^2	1.077
Δρmax, Δρmin(e Å^{-3})	0.168/-0.143

S2-C6	1.657(3)	S1-C1	1.687(3)
S1-C4	1.716(3)	Cl1-C9	1.744(3)
O1-C5	1.222(3)	N2-C6	1.328(4)
N2-C7	1.410(4)	N2-H5	0.78(3)
N3-C5	1.376(4)	N3-C6	1.392(3)
N3-H4	0.87(3)	N1-C9	1.311(4)
N1-C10	1.335(4)	C7-C8	1.381(4)
C7-C9	1.386(4)	C4-C3	1.366(4)
C4-C5	1.459(4)	C8-C11	1.372(4)
C8-H6	0.93	C3-C2	1.400(4)
C3-H3	0.93	C11-C10	1.367(5)
C11-H7	0.93	C2-C1	1.340(4)
C2-H2	0.93	C1-H1	0.93
C10-H8	0.93		

C1-S1-C4	91.31(16)	C6-N2-C7	126.8(3)
C6-N2-H5	116.(2)	C7-N2-H5	117.(2)
C5-N3-C6	128.5(3)	C5-N3-H4	118.2(19)
C6-N3-H4	113.3(19)	C9-N1-C10	116.5(3)
C8-C7-C9	116.7(3)	C8-C7-N2	123.6(3)
C9-C7-N2	119.6(3)	C3-C4-C5	131.4(3)
C3-C4-S1	111.2(2)	C5-C4-S1	117.4(2)
N2-C6-N3	115.1(3)	N2-C6-S2	126.4(2)
N3-C6-S2	118.5(2)	O1-C5-N3	122.1(3)
O1-C5-C4	122.1(3)	N3-C5-C4	115.8(3)
C11-C8-C7	119.0(3)	C11-C8-H6	120.5
C7-C8-H6	120.5	C4-C3-C2	111.9(3)
C4-C3-H3	124.1	C2-C3-H3	124.1
N1-C9-C7	125.3(3)	N1-C9-Cl1	116.0(2)
C7-C9-Cl1	118.7(2)	C10-C11-C8	119.3(3)
C10-C11-H7	120.4	C8-C11-H7	120.4
C1-C2-C3	113.0(3)	C1-C2-H2	123.5
C3-C2-H2	123.5	C2-C1-S1	112.6(2)
C2-C1-H1	123.7	S1-C1-H1	123.7
N1-C10-C11	123.2(3)	N1-C10-H8	118.4
C11-C10-H8	118.4		

Comp.	Stage	DTA peak/^{o}C	TG temp. range/^{o}C	Mass loss%		İnterm. product (or residue)
				Exper.	Theor.	
CoL^{1}_{2}	I	232	145-251	16.2	15.2	$CoL_{5/3}$
	II	295	251-395	12.1	11.4	$CoL_{17/12}$
	III	417	395-587	29.8	30.4	$CoL_{3/4}$
	IV	636	587-830	27.8	29.0	CoS

Comp.	Stage	DTA peak/^{o}C	TG temp. range/^{o}C	Mass loss%		İnterm. product (or residue)
				Exper.	Theor.	
NiL^{1}_{2}	I	223	182-407	15.1	15.2	$NiL_{5/3}$
	II	452	407-583	46.3	45.7	$NiL_{2/3}$
	III	601	583-925	21.2	20.3	NiS_2

Comp.	Stage	DTA peak/^{o}C	TG temp. range/^{o}C	Mass loss%		İnterm. product (or residue)
				Exper.	Theor.	
CuL^{1}_{2}	I	213	145-285	15.2	15.1	$CuL_{5/3}$
	II	320	285-575	45.9	45.3	$CuL_{2/3}$
	III	635	575-935	16.3	15.8	$Cu_{1.96}S$

Comp.	DPPH	ABTS	Red.p.	IC_{50} (ppm)
CoL_2	19,894±0,625	68,248±0,354	8,908±0,843	135
NiL_2	4,9739±0,8882	86,108±0,637	3,3885±0,4895	92
CuL_2	2,283±0,140	1,237± 0,029	0,735±0,067	48

*DPPH, ABTS and reduction power; mg trolax eq./100 mg sample

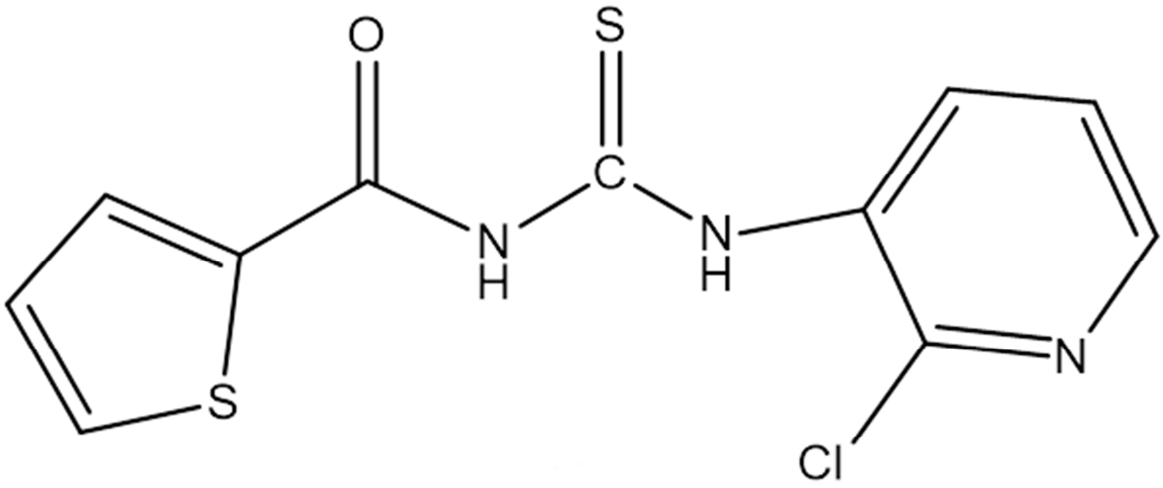

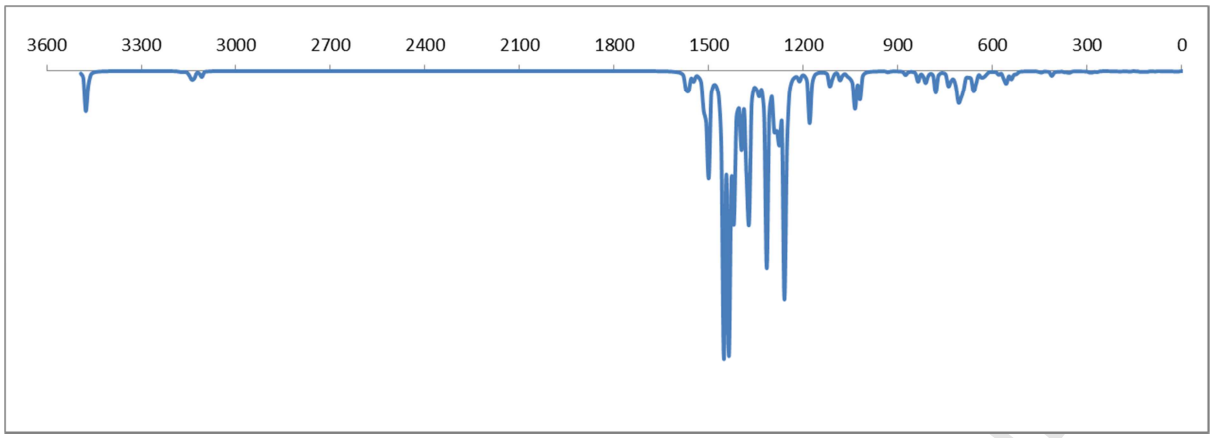

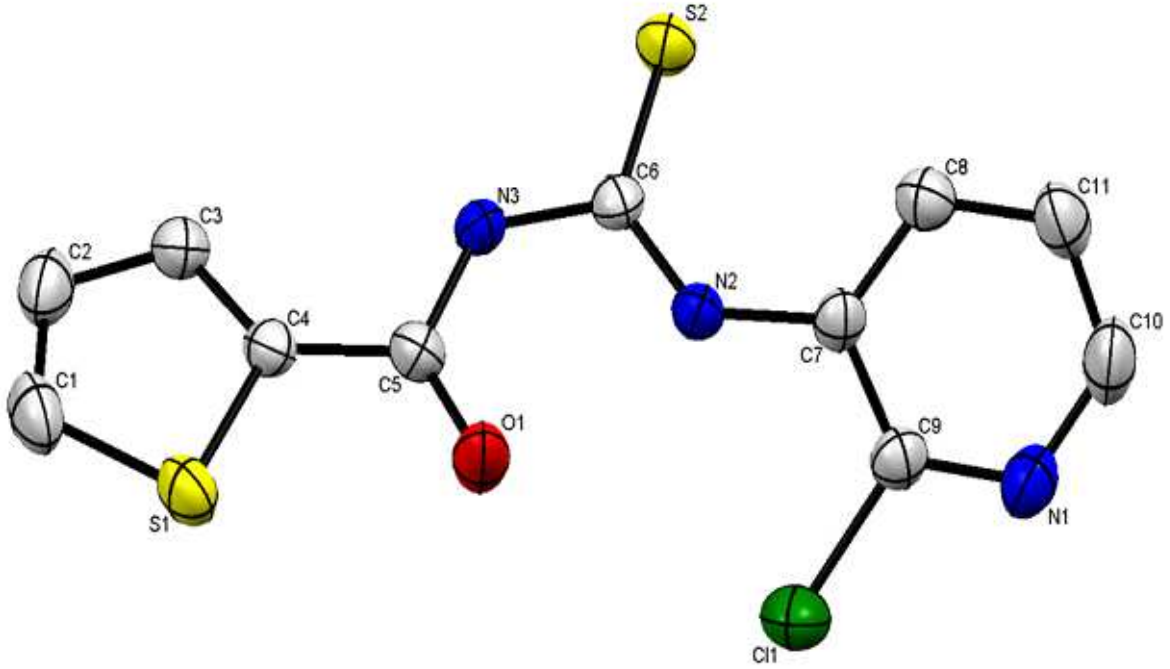

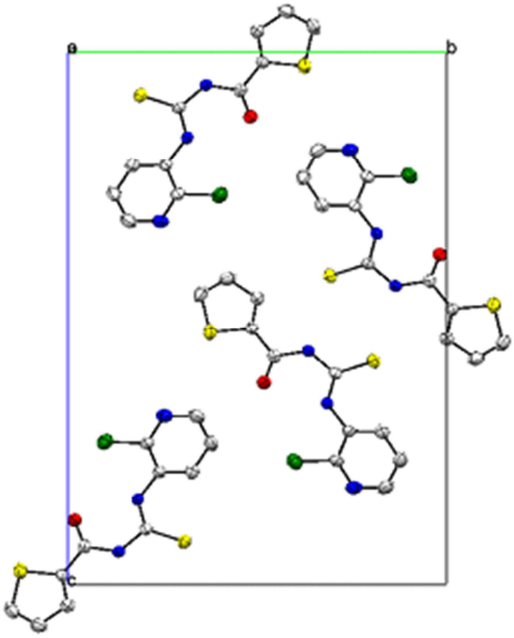

HOMO

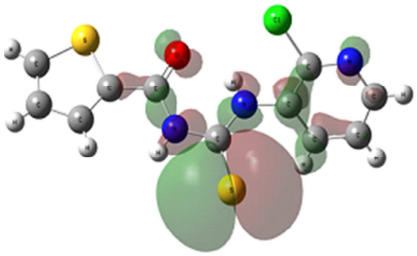

LUMO

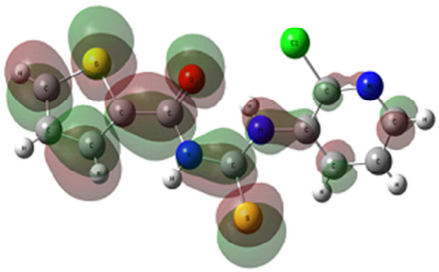

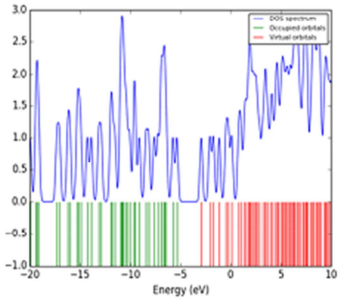

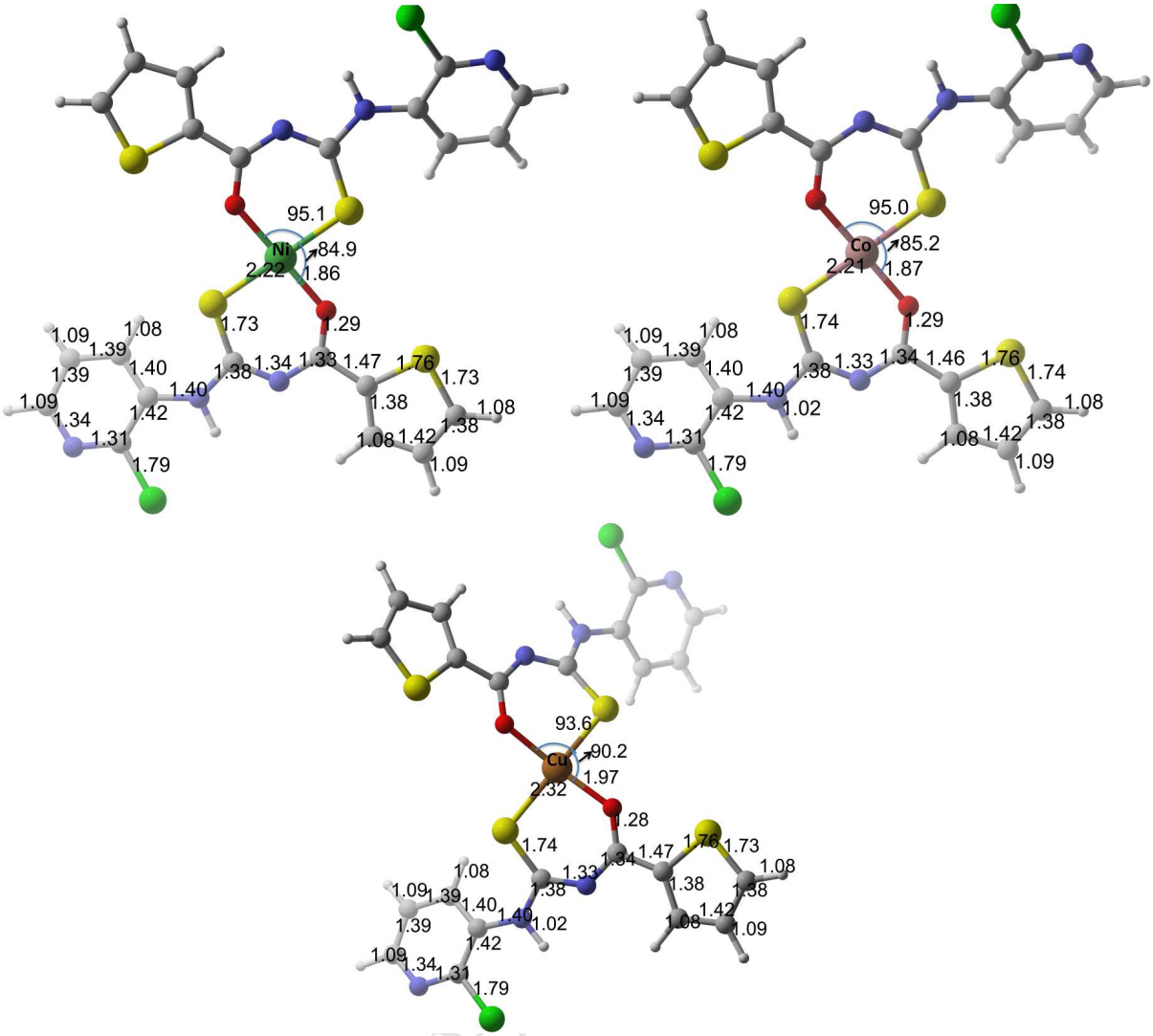
95.1
Ni
84.9
2.22
1.86
1.73
1.29
1.09
1.08
1.39
1.39
1.40
1.09
1.34
1.42
1.31
1.79
1.38
1.34
1.33
1.47
1.76
1.73
1.38
1.08
1.08
1.42
1.38
1.09
95.0
Co
85.2
2.21
1.87
1.74
1.29
1.09
1.08
1.39
1.39
1.40
1.09
1.34
1.42
1.31
1.79
1.40
1.38
1.02
1.33
1.34
1.46
1.76
1.74
1.38
1.08
1.08
1.42
1.38
1.09
93.6
Cu
90.2
1.97
2.32
1.28
1.74
1.08
1.09
1.39
1.40
1.39
1.42
1.09
1.34
1.31
1.79
1.38
1.40
1.02
1.33
1.34
1.47
1.76
1.73
1.08
1.38
1.38
1.08
1.42
1.09